ELSEVIER

Journal of Non-Crystalline Solids 227–230 (1998) 332–337

JOURNAL OF NON-CRYSTALLINE SOLIDS

Section 5. Defects, doparts, impurities

Microscopic nature of localized states in a-Si:H and their role in metastability

S. Yamasaki [a,*], T. Umeda [a], J. Isoya [a], J.H. Zhou [b], K. Tanaka [a]

[a] *Joint-Research Center for Atom Technology, National Institute for Advanced Interdisciplinary Research, 1-1-4 Higashi, Tsukuba-City, Ibaraki 305, Japan*

[b] *Joint-Research Center for Atom Technology, Angstrom Technology Partnership, 1-1-4 Higashi, Tsukuba-City, Ibaraki 305, Japan*

Abstract

Microscopic properties of light-induced electron spin resonance (LESR) centers of $g = 2.004$ and that of metastable dangling bonds ($g = 2.0055$) in undoped a-Si:H have been investigated by means of pulsed electron spin resonance (ESR) techniques. The ^{29}Si hyperfine structure of the $g = 2.004$ signal shows that the wave function of this center spreads mainly over two Si atoms, which suggests that the origin of $g = 2.004$ is electrons trapped at anti-bonding states of weak Si–Si bonds. The microscopic creation mechanism of metastable dangling bonds is discussed on the basis of the frameworks obtained by pulsed ESR.

Keywords: Electron spin resonance; a-Si:H; Wave function

1. Introduction

Hydrogenated amorphous silicon (a-Si) has been widely utilized in the fields of thin film transistors and solar cells. The understanding of localized states in a-Si:H is one of the key issues to improve the device performances. For this purpose, numerous number of studies has been done so far. Electron spin resonance (ESR) is a powerful tool to detect the localized states.

Undoped a-Si:H shows a notorious dangling-bond (DB) ESR signal of $g = 2.0055$. [1] The light-induced metastability is a current topic in a-Si:H and has been attributed to a change in the concentration of the DB ESR signal [1,2]. The understanding of the microscopic mechanism is required from the viewpoint of solar cell applications and is of scientific interest as well. Undoped a-Si:H also shows light-induced ESR (LESR) signals of $g = 2.01$ and $g = 2.004$ under illumination at temperatures less than 100 K, which are ascribed to conduction-band-tail electrons and valence-band-tail holes, respectively [3]. We have detected hyperfine (hf) structures of

* Corresponding author. Present address: Electrotechnical Laboratory, 1-1-4, Umezono, Tsukuba, 305, Japan. Tel.: +81-298 54 2732; Telefax: +81-298 54 2786; e-mail: satoshi@jrcat.or.jp.

[1] $g = h\nu/\beta H_\nu$, where h, ν, and β have their customary meanings and H_ν is the field at which a singularity of a spectral component is observed.

0022-3093/98/$19.00
PII: S0022-3093(98)00333-0

^{29}Si (nuclear spin of $I = 1/2$, natural abundance 4.7%) of the LESR spectrum using a pulsed ESR technique [4]. However, due to the overlapping of two ESR signals of $g = 2.004$ and 2.01 which are broadened by the random orientation and site-to-site variation of structures, the ^{29}Si hf structures could not be deconvoluted into the two independent hf structures, which is necessary for more detailed arguments.

In P-doped a-Si:H, in addition to the tail state signals of $g = 2.004$, a signal with ^{31}P (100% natural abundance, $I = 1/2$) hf structure with 28 mT splitting, which was first reported by Stutzmann and Street [5], appears. They proposed that this component should be ascribed to the electron bound to the donor states. However, from the ESR measurements of P-doped samples with mid-gap Fermi energy, it was found that the location of this state extends down to near the midgap [6,7]. B-doped a-Si:H shows a valence-band-tail signal of $g = 2.01$ [8]. Different from P-doped samples, the 2.01 signal does not show any discernible hf structures related to ^{10}B (19.9% natural abundance, $I = 3$) and ^{11}B(80.1% natural abundance, $I = 3/2$) [9].

In the first part of this paper, we report the deconvoluted LESR spectra of $g = 2.004$ and 2.01 signals in undoped a-Si:H, and analyze the ^{29}Si hf structures of the $g = 2.004$ signal, which shows the experimental evidence of the existence of weak bonds in a-Si:H [10]. In the second part, on the basis of experimental results obtained using a pulsed ESR technique, we discuss the microscopic creation mechanism of metastable DBs [11,12].

2. Experimentals

For detailed study of the LESR spectrum, we used (1) a pulsed ESR technique to obtain a wide-dynamic-range ESR spectrum, (2) an ESR microwave frequency of 11 GHz so that the overlapping of the 2.004 and 2.01 signals should be reduced compared to the case of standard X-band ($\sim$ 9 GHz) measurements, and (3) a sample with increased ^{29}Si content to increase the intensity of ^{29}Si hf structure [13]. In an echo-detected ESR technique, the spectrum is obtained by recording the amplitude of a spin echo signal as a function of magnetic-field strength. To reduce the contribution of the $g = 2.0055$ signal, LESR spectra of $g = 2.004$ and 2.01 were measured at 30 K illuminated by a Ti-sapphire laser ($h\nu = 1.7$ eV, output power = 30 mW/cm^2). Under those conditions, the peak height of the LESR spectrum was more than 20 times larger than that of the dark ESR spectrum (DB) in the range of 10^{15} cm^{-3} in these samples.

3. Results

Fig. 1 shows the LESR spectra of the samples with different contents of ^{29}Si ([^{29}Si] = 9.1, and 4.7 at.%), which were recorded using a two-pulse Hahn-echo detected ESR technique (90° pulse–τ–180° pulse–τ-echo, $\tau = 240$ ns, repetition time of a pulse sequence, RT = 10 ms) [14]. The linewidth is broadened by the increase of ^{29}Si content, which means that the weak hf interactions with distant ^{29}Si contributes to the linewidth of the $g = 2.004$ signal. In the magnetic-field range > 392.5 mT, a long tail is noted, and its intensity increases with increase of ^{29}Si. The ratio of the integrated area of the tail structure to the total area was found to be proportional to the ^{29}Si content (Fig. 2), clearly indicating that the tail structure originates from the higher-field side peak of the ^{29}Si hf doublet. This identification has confirmed that of our previous report [4].

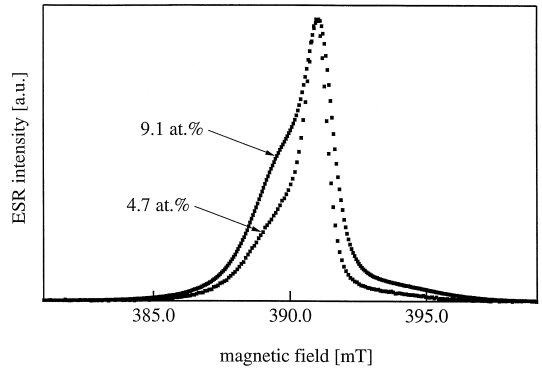

Fig. 1. LESR spectra at 30 K of undoped a-Si:H with [^{29}Si] = 9.1, 4.7 at.%, which were recorded by two-pulse Hahn echo-detected ESR technique ($\tau = 240$ ns, RT = 10 ms, the microwave frequency 10.98 GHz). The spectra were normalized to their peak heights.

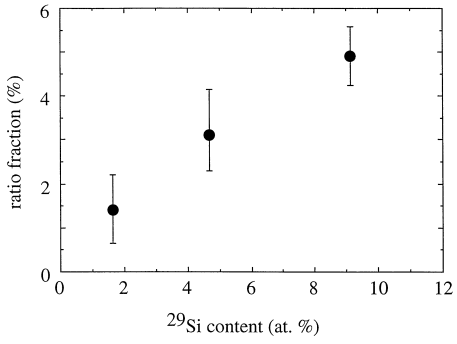

Fig. 2. The intensity of the tail structure on the high-field side as a function of [^{29}Si]. The ratio fraction relative to the total area of the whole ESR spectrum is given.

We have studied a variety of spin-relaxation behaviors of both signals using pulsed ESR [10]. Eventually, we have found that the spin-lattice relaxation time of the components (T_1) differs. The T_1 for $g = 2.004$ and 2.01 were determined to be 1.3 ms and 0.47 ms at 30 K, respectively. Thus, the T_1 of $g = 2.01$ is about one third of that of $g = 2.004$.

Deconvolution of the two overlapping LESR signals of $g = 2.004$ and 2.01 has been achieved by using the difference in T_1 between the two signals. When we use a short RT of 0.5 ms for two-pulse Hahn-echo detected ESR, the 2.01 signal becomes relatively stronger than the 2.004 signal because the reduction of the echo intensity due to partial recovery is larger in the 2.004 signal than in the 2.01 signal. On the other hand, when we adopt a three-pulse stimulated echo (90° pulse–τ–90° pulse–τ'–90° pulse–τ-echo, $\tau = 240$ ns, RT = 10 ms) for measuring the echo-detected ESR, the 2.01 signal is relatively suppressed by using a long τ' of 1 ms, because the decay time of the stimulated echo signal with respect to τ' corresponds to T_1. In this way, by using two different pulse sequences, we obtained two echo-detected ESR spectra with different relative intensities between 2.01 and 2.004 signals. The LESR spectrum of the ^{29}Si-enriched (9.1 at.%) sample was deconvoluted into two independent spectra by subtracting one from the other to cancel out either the 2.004 or the 2.01 signal alternatively, which subtraction is shown in Fig. 3.

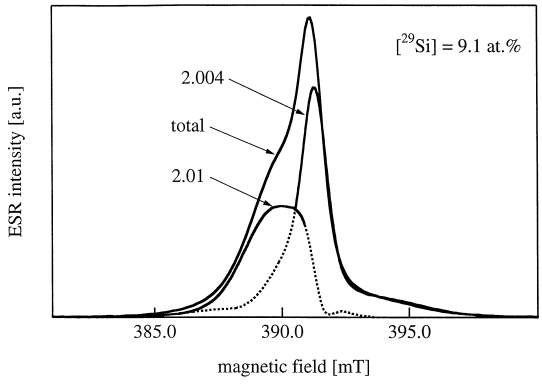

Fig. 3. Deconvoluted spectra of the LESR ($g = 2.004$, 2.01) of the ^{29}Si-enriched (9.1 at.%) undoped a-Si:H. Solid lines indicate the deconvoluted 2.004 and 2.01 spectra with a high reliability in data analyses, while dashed lines include some ambiguity.

4. Discussion

4.1. Electronic structure of band-tail electrons in a-Si:H

Although the center part of the spectrum could not be deconvoluted due to the overlap of the two signals, the hf structure observed on the high-field side belongs mainly to the $g = 2.004$ signal, as is seen in the figure. The area of the high-field-side hf structure, which should correspond to one-half of the area of the entire hf structure ($I = 1/2$), was estimated to be $20 \pm 3\%$ of one-half of the total area of the $g = 2.004$ signal, being almost twice the ^{29}Si abundance (9% for the sample used here). This magnitude is quite different from the case of a DB signal ($g = 2.0055$), in which the ratio is almost the same as the ^{29}Si abundance ratio. The area fraction of the hf structure depends on the number of Si atoms, N, on which an electron spin is mainly located. By the quantitative discussion, we conclude that the wave function of the 2.004 center spreads mainly over two Si atoms [10].

In an amorphous network, it is quite possible that largely elongated covalent bonds (weak bonds) are present and give rise to energy levels in the tail regions of the conduction and valence bands. In this case, when an electron is trapped in an anti-bonding state, its wave function is expected to extend over the two Si atoms associated with the weak Si–Si

bond. Consequently, the present results suggest that the origin of the LESR signal of $g = 2.004$ is electrons trapped at weak Si–Si bonds whose anti-bonding states are located at the conduction-band tail. Recently, the LESR signal has been measured as a parameter of light intensity, which shows that the hf coupling is almost unchanged in spite of the change of quasi-Fermi energy due to the change of light intensity. This suggests that the electronic state of $g = 2.004$ signal is decreased and located at a unique energy compared to that of an empty state. The details are described in the another paper in this volume [13].

4.2. Metastable dangling bonds

4.2.1. Experimental evidence of metastable DB

To understand the microscopic creation mechanism of the metastable DBs, many works have been done using continuous-wave (CW) ESR technique. Although a change of DB densities by light illumination was easily observed by CW-ESR, no spectral change between after and before light illumination was detected by CW-ESR. Although CW-ESR might seem to be incapable of elucidating microscopic structure of the metastable DBs, it supplies us some important insights.

Hydrogen nearby an electron spin should be evidenced from the change in an ESR spectrum which is expected from the difference of hf interaction by replacing hydrogen atoms ($I = 1/2$, $g_n = 5.5856912$) by deuterium atoms ($I = 1$, $g_n = 0.8574376$). However, the effect of deuteration on the linewidth was not detected for the case of metastable DBs of a-Si:H in the X-band ESR spectrum [14,15].

An electron spin experiences a dipolar field from a nearby nuclear spin. The hf interaction due to dipole–dipole interaction (in mT) is given by:

$$A_{\mathrm{dip}}/g\beta_{\mathrm{e}} = g_n\beta_n(3\cos^2\theta - 1)/r^3, \qquad (1)$$

where β_{e} and β_{n} are the Bohr magneton and nuclear magneton, respectively, θ the angle between the external field and the vector from an electron spin to a nuclear spin, r the distance between electron and nuclear spins. At $r = 3$ Å, $g_n\beta_n/r^3$ is 0.1045 mT and 0.0160 mT for hydrogen and deuterium, respectively. Therefore, if DBs accompany hydrogen at a distance smaller than 3 Å, the CW-ESR linewidth should be affected by deuteration, because the linewidth change by 0.1 mT is detectable for a DB spectrum with the linewidth of 0.7 mT. It is concluded that the metastable DB does not form a complex accompanied by a hydrogen atom within 3 Å.

For more detailed check, we performed the L-band (1.06 GHz) ESR experiments, since, by changing from conventional X-band (9 GHz) to L-band, the line broadening originating from g-value distribution should be reduced by a factor of nine while the line broadening due to hf interaction is unaffected. L-band ESR spectra of a-Si:H deposited at room temperature were measured as a function of post-annealing temperatures, in which the spin density of the sample was varied from 2×10^{18} down to 1×10^{17} cm^{-3} (Fig. 4). Every measured spectrum shows a single sharp peak and no characteristic feature due to a hf structure originating from close hydrogen was observed, which suggests that DBs with a strong ^{1}H hf interaction are very few if exists and that major DBs are spatially located in a hydrogen-depleted region. This result is quantitatively consistent with the results obtained from electron-spin-echo envelope-modulation of pulsed ESR [11,12]. Quite recently, Stutzmann reported using the high resolution spin resonance spectra obtained by low-field spin-dependent transport that no close hydrogen atoms were detected around the metastable DB [16]. Our result of L-band ESR is consistent with his report.

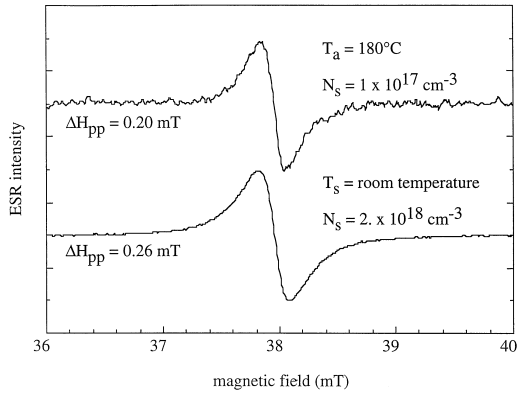

Fig. 4. L-band CW-ESR spectrum of the DB ($g = 2.0055$) of undoped a-Si:H.

The distance between metastable DBs is also important information required for understanding its creation mechanism, because the bond breaking, which is a simple way to create DBs in an a-Si:H network, makes a pair of DBs simultaneously. For the closest pair case, where there is an overlapping of wave functions between a pair of DBs, an exchange narrowing effect is usually expected. However, we confirmed there is no exchange narrowing effect in metastable DBs using ^{1}H-ENDOR detected ESR spectrum as well as using pulsed ESR [17]. The other interaction between two electron spins of a pair is a dipole–dipole interaction. When an electron spin of A is located in the vicinity of another electron spin of B, the dipolar field at the position of A due to the B spin is expressed as:

$$B_{\mathrm{dip}}/g\beta_{\mathrm{e}} = M_{\mathrm{s}}\, g\beta_{\mathrm{e}}(1-3\cos^2\theta)/R^3, \qquad (2)$$

where θ is the angle between the external field and the vector from B spin to A spin, R the distance between B spin and A spin. The dipolar field around 1 mT is roughly equivalent to a 10 Å spin–spin separation (At $r = 10$ Å, $g\beta_{\mathrm{e}}/R^3$ is 1.86 mT), which must clearly be detected in the CW-ESR spectra of a-Si:H [18], since the peak-to-peak width of a DB signal in a-Si:H is around 0.7 mT. This points out that the metastable DBs are separated each other at least by 10 Å.

In order to obtain more detailed microscopic information than that obtained from a CW-ESR spectrum, we have used a pulsed ESR technique which can extract a small hf interaction with surrounding nuclei as well as a small dipole–dipole interaction with surrounding electron spins. The experimental results have pointed out the frameworks for understanding the microscopic mechanism of metastable DBs in a-Si:H. Although there is no space to describe details, the important experimental results are just summarized as:

1. No DB–H complex in which DB accompanies hydrogen at specific close distance has been detected.
2. No DB pair has been detected (metastable DBs are distributed randomly with the average separation between DBs larger than 400 Å).

The details were described in the references of Refs. [11,12,19].

4.2.2. Microscopic creation mechanism of metastable DB

A simple way to create DBs in an a-Si:H network is breaking of weak Si–Si bonds. Many models involving Si–Si bond breaking have been proposed. In order for two DBs to be stabilized in the network and to avoid restoring to the original Si–Si bonding, bond switching mechanisms have been proposed and are shown in Fig. 5a–e [20–24]. For these cases, except (d) involving floating bonds and (e) involving a volume rearrangement caused by the change of the localized state independent of hydrogen atoms,

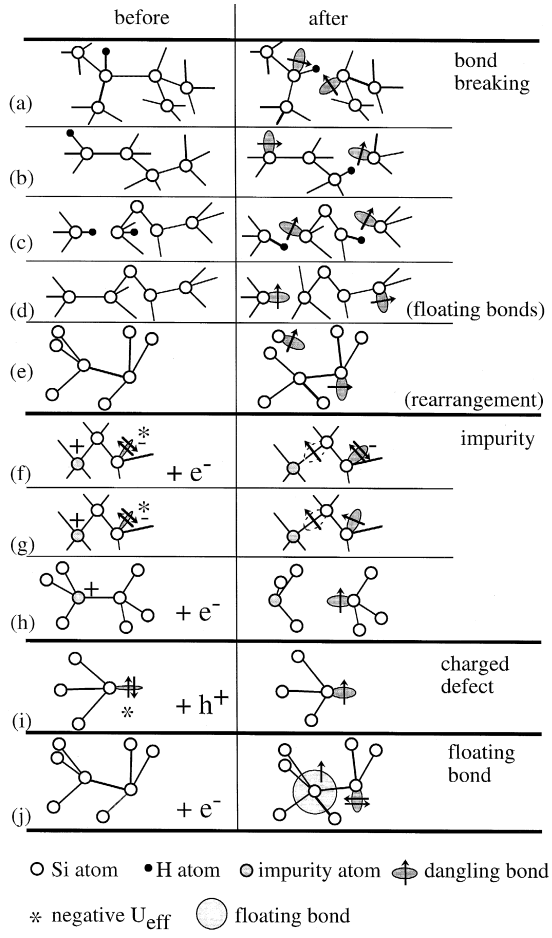

Fig. 5. Models for the creation mechanism of the light-induced metastable DBs. The references are (a) Ref. [20], (b) Ref. [21], (c) Ref. [22], (d) Ref. [23], (e) Ref. [24], (f) Ref. [25], (g) Ref. [26], (h) Ref. [27], (i) Ref. [34], and (j) Ref. [33].

metastable DBs (at lease one of two DBs) are forming DB–H complexes. However, as the experimental results of 1, these DB–H complexes have been excluded by the pulsed ESR study.

For bond breaking models of (a)–(e), two DBs are simultaneously created. In the models of (d), two DBs spatially separate each other through high mobility of the floating bonds after bond breaking of weak Si–Si bonds. The models of (a)–(c) and (e) form intimate DB pairs. However, from the experimental result of 2, these models are unlikely.

On the other hand, the models related with impurities such as oxygen, nitrogen, carbon, and phosphorus atoms have been proposed [25–29]. The pulsed ESR technique can provide the detailed information of the spatial relationship between an electron spin and its adjacent nuclear spins. However, we could not detect any relationship with impurities of ^{14}N, ^{17}O, and ^{13}C using ^{17}O and ^{13}C enriched samples [30]. The CW-ESR measurements using samples with quite low oxygen and carbon content also pointed out that there is no relationship between metastable DB and impurities [11,31,32].

The models involving floating bond of (e) and (j) [33], and charged DBs with negative effective-correlation-energy of (i) [34] do not conflict with the frameworks of 1 and 2. However, the existence of floating bonds and charged DBs themselves has not been experimentally confirmed so far. Although the microscopic structure has been understood step by step, we need new experimental evidence to obtain the perfect understanding of the microscopic origin of metastable DBs in a-Si:H.

References

[1] I. Hirabayashi, K. Morigaki, S. Nitta, Jpn. J. Appl. Phys. 19 (1980) L357.
[2] H. Dersch, J. Stuke, J. Beichler, Appl. Phys. Lett. 38 (1981) 456.
[3] J.C. Knights, D.K. Biegelsen, I. Solomon, Solid State Commun. 22 (1977) 133.
[4] S. Yamasaki, H. Okushi, A. Matsuda, K. Tanaka, J. Isoya, Phys. Rev. Lett. 65 (1990) 756.
[5] M. Stutzmann, R.A. Street, Phys. Rev. Lett. 54 (1985) 1836.
[6] S. Yamasaki, S. Kuroda, H. Okushi, K. Tanaka, J. Non-Cryst. Solids 77–78 (1985) 339.
[7] S. Schutte, F. Finger, W. Fuhs, J. Non-Cryst. Solids 114 (1989) 411.
[8] H. Dersch, J. Stuke, J. Beichler, Phys. Stat. Sol. B 107 (1981) 307.
[9] S. Yamasaki, S. Kuroda, J. Isoya, K. Tanaka, J. Non-Cryst. Solids 97–98 (1987) 691.
[10] T. Umeda, S. Yamasaki, J. Isoya, A. Matsuda, K. Tanaka, Phys. Rev. Lett. 77 (1996) 4600.
[11] S. Yamasaki, J. Isoya, J. Non-Cryst. Solids 164–166 (1993) 169.
[12] J. Isoya, S. Yamasaki, H. Okushi, A. Matsuda, K. Tanaka, Phys. Rev. B 47 (1993) 7013.
[13] T. Umeda, S. Yamasaki, J. Isoya, A. Matsuda, K. Tanaka, in this volume.
[14] J. Isoya, S. Yamasaki, A. Matsuda, K. Tanaka, Phil. Mag. B 69 (1994) 263.
[15] D.K. Biegelsen, M. Stutzmann, Phys. Rev. 33 (1986) 3006.
[16] M. Stutzmann, in: M. Hack, E.A. Schiff, R. Schropp, I. Shimizu, S. Wagner (Eds.), Amorphous and microcrystalline silicon technology 1997, Mater. Res. Soc. Proc., 467, Pittsburgh, PA, 1997, in press.
[17] S. Yamasaki, M. Kaneiwa, S. Kuroda, H. Okushi, K. Tanaka, Phys. Rev. B 35 (1987) 6471.
[18] H. Dersch, J. Stuke, J. Beichler, Appl. Phys. Lett. 38 (1981) 456.
[19] S. Yamasaki, J. Isoya, K. Tanaka, to be submitted in Phys. Rev.
[20] M. Stutzmann, W.B. Jackson, C.C. Tsai, Phys. Rev. B 34 (1986) 63.
[21] K. Morigaki, Jpn. J. Appl. Phys. 27 (1988) 163.
[22] W.B. Jackson, Phys. Rev. B 41 (1990) 10257.
[23] T. Shimizu, M. Kumeda, Jpn. J. Appl. Phys. 35 (1996) L816.
[24] P.A. Fedders, Y. Fu, Phys. Rev. Lett. 68 (1992) 1888.
[25] H. Okushi, R. Banerjee, K. Tanaka, in: H. Fritzsche (Ed.), Amorphous Silicon and Related Materials, World Scientific, 1989, p. 657.
[26] N. Ishii, M. Kumeda, T. Shimizu, Jpn. J. Appl. Phys. 24 (1985) L244.
[27] D. Redfield, R.H. Bube, Phys. Rev. Lett. 65 (1990) 464.
[28] H. Fritzsche, J. Non-Cryst. Solids 190 (1995) 180.
[29] G. Lucovsky, M.J. Williams, S.M. Cho, Z. Jing, J.L. Whitten, Mater. Res. Soc. Symp. Proc. 336 (1994) 275.
[30] S. Yamasaki, I. Umeda, J. Isoya, A. Matsuda, K. Tanaka, in: M. Hack, E.A. Schiff, S. Wagner, R. Schropp, A. Matsuda (Eds.), Amorphous Silicon Technology 1996, Mater. Res. Soc. Proc., 420, Pittsburgh, PA, 1996, p. 587.
[31] T. Kamei, N. Hata, A. Matsuda, T. Uchiyama, S. Amano, K. Tsukamoto, Y. Yoshioka, T. Hirao, Appl. Phys. Lett. 68 (1996) 2380.
[32] M. Nakata, S. Wagner, T.M. Peterson, J. Non-Cryst. Solids 164–166 (1993) 179.
[33] T. Pantelides, Phys. Rev. B 36 (1987) 3479.
[34] D. Adler, Solar Cells 9 (1983) 133.